Current Opinion in Colloid & Interface Science 18 (2013) 481–492

Contents lists available at ScienceDirect

Current Opinion in Colloid & Interface Science

journal homepage: www.elsevier.com/locate/cocis

Cell adhesion promotion strategies for signal transduction enhancement in microelectrode array *in vitro* electrophysiology: An introductory overview and critical discussion ☆

Axel Blau *

Fondazione Istituto Italiano di Tecnologia, Dept. of Neuroscience and Brain Technologies, Neurotechnologies Unit, Via Morego 30, 16163 Genoa, Italy

ARTICLE INFO

Article history:
Received 12 June 2013
Received in revised form 3 July 2013
Accepted 8 July 2013
Available online 20 July 2013

Keywords:
Microelectrode array (MEA) electrophysiology
Electrical signal transduction
Interfacial contact
Interfacial biopatterning technologies
Guidance cues
Extracellular matrix (ECM)
Cell adhesion

ABSTRACT

Microelectrode arrays (MEAs) find application both *in vitro* and *in vivo* to record and stimulate electrical activity in electrogenic cells such as neurons, cardiomyocytes, pancreatic beta cells or immortalized cell lines derived therefrom (*e.g.*, PC12, HL-1). In MEA electrophysiology, the quality of the predominantly extracellularly recorded or elicited electrical signals strongly depends on the distance, strength and stability of the interfacial contact between the electrogenic cells and an electrode. Decorating the substrate or electrode with biochemical adhesion factors and physical guidance cues does not only determine the tightness of that junction, but it also modulates substrate biocompatibility, its biostability, cell differentiation as well as cell fate. If an interface is furthermore topologically, chemically or physically patterned or constrained, neural interconnectivity may be steered towards directional organization. In this introductory and selective overview, we briefly discuss adhesion events at the chemical and biological level, review the general role and mechanisms of cell adhesion in (neuro)biology, then explore how cells adhere to artificial substrates. This will lead to the discussion of popular strategies for enhancing and steering interfacial interactions at the bio-hardware boundary with particular focus on MEA substrates. It will include a critical treatment of open issues with respect to the origin and shape of extracellularly recorded signals and their modulation by cell-culture-inherent events.

1. Introduction

Stickiness is very likely one of the key factors that drove the development and evolution of complex life [1]. Not surprisingly, adhesive interactions of membrane-bound molecular ensembles are a prerequisite for survival of almost all multicellular organisms on earth. Therefore, the majority of cells in a multicellular organism are anchorage-dependent with the exception of hematopoietic cell lines. This overview briefly reviews the various functions of cell adhesion and its particular role in neurobiology. It will then focus on chemical events at artificial interfaces in contact with solvents and biology. Because of the large mismatch between chemical, biomechanical and textural properties of cells and synthetic devices such as microelectrode arrays (MEAs), it is quite challenging to establish a stable and functionally predictable interfacial interaction between the two. We will therefore look at the most common strategies for controlling adhesion chemistry and surface texture of interfaces to render them more biomimetic. In a best-case scenario, cells should not notice being removed from their natural tissue environment. We will then discuss the particular requirements for and events at chemically and topographically inhomogeneous MEA interfaces and review suitable chemical and physical strategies for controlling adhesion and directional neural development on these devices. MEAs are particularly demanding because, with few exceptions, the overall electrode density is sparse. We will therefore examine a few prominent examples of placing neurons directly onto electrodes or guiding their neurites across. As we proceed, we will discuss how the relative position and tangency of the cell membrane and the electrode critically determine signal amplitude and stability, and the consequential implications for the theoretical description and modeling of the cell-electrode-junction.

2. The role of the extracellular matrix (ECM)

Besides soluble signaling molecules (hormones, cytokines and other growth factors), adherent cell types secrete, depending on their developmental stage, various types of soluble proteins that intercalate into a mesh of insoluble collagen fibers. This tissue-specialized extracellular matrix (ECM) plays a key role in tissue homeostasis, cell attachment, growth, proliferation, differentiation, morphology, polarization, directional motility, migration and cell spreading [2•]. Its constituents exist in multiple, interconvertible forms that are constantly remodeled in response to changes in ECM properties, cytoskeletal organization, cell

* Tel.: +39 010 7178 1729; fax: +39 010 7178 1230.

1359-0294/$ – see front matter © 2013 The Author. Published by Elsevier Ltd. All rights reserved.
http://dx.doi.org/10.1016/j.cocis.2013.07.005

development, migration and signaling processes [3•]. Depending on their timing, physicochemical protein-receptor mediated cell–cell and cell-matrix interactions may trigger a particular cellular process or signaling cascade, thereby steering a wide range of cellular functions that may determine stem cell fate and orchestrate the development of multicellular organisms. In contrast, the absence of such interactions may functionally lock a cell, thereby leading to senescence or apoptosis. In the brain the ECM affects structural and functional plasticity and acts as a degradable stabilizer of neural microcircuits. For instance, its activity-dependent modification supports the formation of dendritic filopodia and the growth of dendritic spines. ECM molecules further play a role in learning and memory by regulating various aspects of synaptic plasticity, scaling synaptic responses, stabilizing synaptic connectivity, directing axonal outgrowth and regulating the development of myelinating glia. For details on ECM constituents, their biochemistry, functional diversity (*e.g.*, types and structures of proteins, action mechanisms, associated intracellular events) and dynamics, the reader is referred to recent all-encompassing reviews and protocols [4•,5•].

3. The need for ECM mimicry at artificial interfaces — From macro to micro, from (bio)chemistry to (bio)physics to material sciences

As indicated, the interface between the cell and its environment, especially the ECM, has a profound effect on cell phenotype and fate. While some cells are able to synthesize all required ECM components, others require an exogenous source, particularly when grown in serum-free culture [6]. In consequence, if cells are supposed to get into contact with foreign materials such as implants or in cell culture, the interfaces of these objects have to meet certain criteria for mimicking the extracellular environment of the host as best as possible. In addition to imitating ECM properties, artificially-tailored functionalization by chemical, topological or structural cues can serve the purposeful programming of cells. This allows for driving cellular events such as gene expression into desired directions, for instance to express a certain phenotype or impose a preferred growth or differentiation directionality [7••]. Therefore, much research has been invested into altering the chemical, topographical and elastomechanical properties of non-biological substrate surfaces that are supposed to get into contact with cells or tissue [8•]. In a complex interplay, parameters such as the bio- and physicochemical properties of a surface (*e.g.*, functional groups, surface charge, surface pH, hydrophobicity, exposed ligands), its micro-, nano- and ultrastructure ('function follows form') [9•], the existence of gradients [10•], as well as material porosity, its compartmentalization and biomechanical properties (*e.g.*, stiffness, compliance) [11••,12•] play decisive and not necessarily synergistic roles in the type and effect of a cell-hardware interaction [13••]. This is the case for both adhesive and anti-adhesive surfaces. As an example, Lensen et al. have demonstrated that adhesion-aversive chemical material properties can be compensated and overwritten by topographic adhesion cues [14]. In a different context, an often-cited example is wax that tends to be sticky. However, arranged in a hierarchical microtopography of papillae covered by epicuticular nanostructured waxes on the Lotus leaf, it takes functional part in a water and dirt-repellent mechanism (Lotus effect) [15].

Adhesion is by no means static. Passive changes in local chemistry (*e.g.*, pH) due to the accumulation of metabolites or the cellular secretion of enzymes may chemically alter adhesiveness and thus weaken the interaction. However, depending on their needs or bodily function, cells can also actively modulate adhesion locally. Just as animals, when clinging to something, can let go at any time to not be permanently trapped, cells can control transitory attachment and detachment processes during locomotion or lamellipodial and filopodial exploration of their environment. Research into switchable surfaces aims at taking over control [16•].

3.1. Chemical adhesion events at a bio-hardware interface

Adhesion refers to the phenomenon of interfacing entities that experience intermolecular attractive forces of strengths between 0.5 and 400 $kJ \cdot mol^{-1}$ at distances between 2 and 85 Å. These entities can be gasses, liquids, solids or any permutation of the three. As a result, interfaces tend to become 'dirty' very easily, and it is not always easy to get and keep them clean. A surface (adsorbent) readily adsorbs molecules (adsorbates) from all three phases (gaseous, liquid or solid). A solid–solid contact allows the transfer of bulk material, and adsorption from the gas phase leads to the progressive growth of the deposited layer thickness. In contrast, at a solid–liquid interface, a particular substance will usually deposit as a monolayer because, once in surface contact, it screens the original interface properties and thus prevents further build-up. The newly exposed surface chemistry then allows compounds with different affinities to deposit on top of such monolayer. However, in almost all cases the composition of an adsorbed layer will change over time due to the different desorption kinetics and surface mobilities of the various adsorbates; molecules or proteins with higher affinity for the surface thereby displace faster diffusing molecules (Vroman effect). The surface chemistry and (nanometer) morphology will also decide on the conformational and thus functional destiny of an ECM component [17••]. Proteins will not only change their conformation upon adsorption to minimize their free energy, thereby redistributing charged groups, dehydrating both the sorbent surface and part of the protein surface, and reorganize intramolecular H-bonds. They also dynamically rearrange and refold upon experiencing chemical changes in their vicinity. Other than being one of the reasons why interface-bound proteins hardly ever detach from surfaces again, it also explains why their functionality may be altered by either distorting or hiding the adhesion-mediating motive or, on the contrary, by enhancing its accessibility [18•]. In addition, biochemical coatings tend to change or degrade due to changes in the chemical microenvironment (*e.g.*, pH) or simply by being digested by the cells on top of them.

3.2. Chemical events at a liquid–solid interface

Water is a good solvent for its high dielectric constant, particularly for ions. Therefore, a solid-aqueous interface is quite reactive even in the absence of adsorbates. The interface can become charged also at physiological pH by picking up protons (*e.g.*, exposed amino groups of proteins) or losing them upon the dissociation of hydroxyl groups (*e.g.*, oxides). Driven by the concentration gradient or the gradient in the electrochemical potential, a surface may also partially dissolve. In a short time, local distribution gradients for solutes will form and, if surface charges are present, an inner electric double layer in close contact with the solid surface (Helmholtz layer) as well as a diffuse layer on top of it (Gouy-Chapman layer) (Fig. 1 left). The two gradients may not necessarily have the same trend or profile. This in turn will influence the interface adsorption tendency for a particular species of dissolved compounds.

3.3. Adhesion-mediating compounds and mechanisms

The extracellular side of most animal cell membranes carries a net negative charge due to a dense and confluent negatively-charged network of proteoglycans, glycolipids and glycoproteins, which contribute to cell–cell recognition, communication and intercellular adhesion (Fig. 1 right). Its charge density has been estimated to be $-18 \cdot 10^{-3}\ Cm^{-2}$ [19]. This glycocalyx allows the body to distinguish between its own cells and transplanted tissues, diseased cells or invading organisms.

This has been exploited early on for binding (at physiological pH) cationic polyamino acids like poly(lysine) (PL), poly(ornithine) (PO), poly(arginine), and poly(ethylenimine) (PEI) to the surfaces of animal cells to either immobilize them, extract their membranes or coat

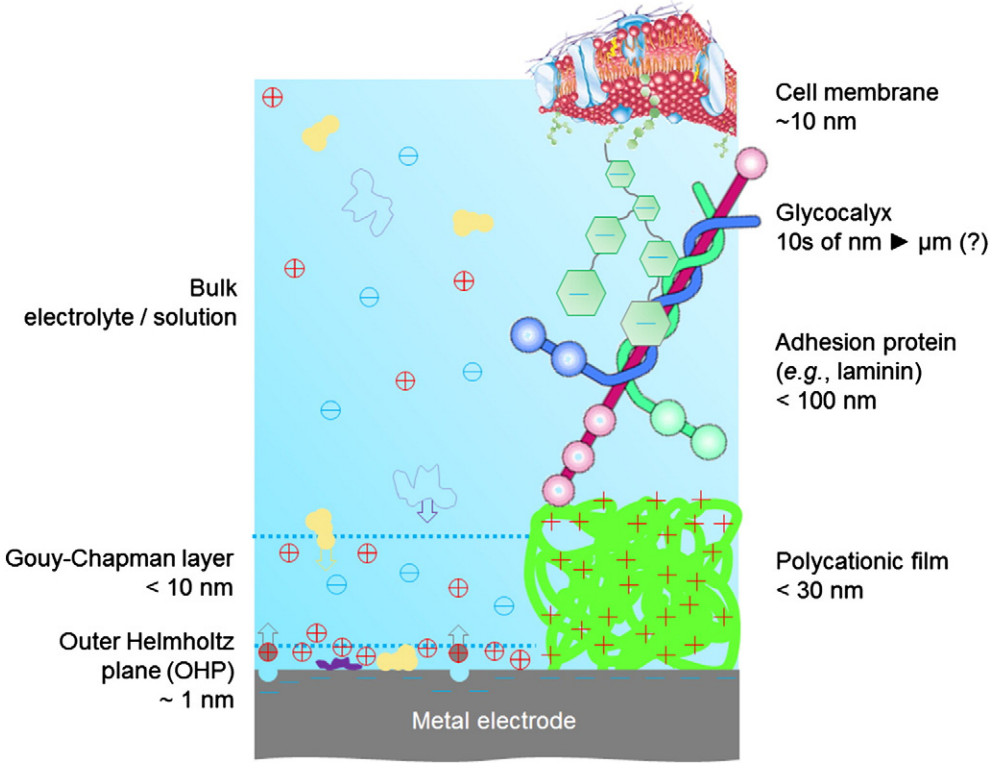

Fig. 1. Chemical events at a liquid–metal interface (left) and relative thicknesses of adhesion-mediating films, ECM- and membrane components (right). A metal electrode can partially dissolve along the electrochemical potential, thereby releasing metal cations into the solution. Charged and neutral particles (yellow) as well as dissolved components (violet) can precipitate from the solvent onto the substrate. Depending on their interaction energies and desorption kinetics, they may turn back into the bulk solution after some time. Hydration sheaths were omitted to enhance clarity. According to recent findings by means of fluorescence infiltration studies [67] and rapid freezing/freeze substitution (RF/FS) transmission electron microscopy (TEM) [68], the negatively charged glycocalyx and in consequence the cleft between substrate and cell membrane are orders of magnitude thicker than previously thought. This may affect ion flux, seal resistance and in consequence signal amplitude and shape of extracellularly recorded membrane potential fluctuations.

implants with multilayers of oppositely charged polyelectrolytes. Commercially available polyamino acids like poly-L-lysine (PLL), poly-D-lysine (PDL) and poly-L-ornithine (PLO) with molecular weights between 30 and 300 kDa are usually deposited from 0.01% solution [20]. However, depending on their identity, chirality (D *versus* L isomers) and molecular weight, polycations have different competitive modes of actions and toxicity, which may vary with cell type. For instance, polycations of low-molecular weight (2.8 kDa) support the uptake of proteins and single and double-stranded polynucleotides into the cell as non-viral transfection agents [21]. Polycations of middle and long-chain length and high molecular weight (170 kDa) turned out to be cytotoxic already at low concentrations (10 µg/ml) [22]. Recent studies suggest that apart from molecular weight, the concentration, exposure time, structure and cationic charge density of a polymer not only determine adhesion strength, but also cell damage [23]. For the particular example of polycations as gene delivery vehicles, cytotoxicity in the form of membrane damage was found to decrease in the following order: poly(ethylenimine) (PEI) = poly(L-lysine) (PLL) > poly(diallyldimethyl-ammonium chloride) (DADMAC) > diethylaminoethyl (DEAE)-dextran > poly(vinyl pyridinium bromide) (PVPBr) > Starburst (PAMAM) dendrimer > cationized albumin > native albumin. In addition, film thicknesses may depend on pH during film preparation (*e.g.*, 200% swelling at physiological pH 7.4 if prepared at acidic pH) [24].

Different polycations and their enantiomers also show different long-term stabilities with respect to their adhesion-mediating propensity in cell culture. Besides enantiomer-specific digestion by some cell types (*e.g.*, PLL is more easily digested than PDL [20]), there is little knowledge on other degradation or chemical masking mechanisms, and how they depend on the type of substrate, its porosity, topography and pre-treatment (*e.g.*, plasma-exposure, corona discharge), coating protocol, cell type and medium composition. Indicators are cell carpet detachment or ignorance of patterned cell confinement areas. It is furthermore likely that films get 'conditioned' over time and thus change their biochemical properties and functionality by chemical components and environmental parameters (*e.g.*, pH, ionic composition, T).

It is difficult to predict or explain whether and why for instance a PDL adhesion layer will not always be functional for all users despite them following the same deposition protocol. Small differences in handling or substrate preparation may be the main reason. This is particularly surprising because there are several very different deposition protocols that lead to equally functional adhesion layers: *e.g.*, the incubation of a drop of a polyamino acid solution on a substrate for a few hours or overnight in a humidified incubator, or the immediate drying of such drop in vacuum at room temperature. In all protocols, though, thorough rinsing with sterile water or phosphate buffered saline (PBS) following the deposition is mandatory in order to remove non-physisorbed polymer fragments, which tend to be toxic for neurons.

The ECM can be regenerated in an organism, but less efficiently in cell culture. Therefore, polycations are typically combined with proteins from the basement membrane matrix of the ECM such as laminin, fibronectin (FN), vitronectin (VTN) and collagen, (N)-cadherin, neural cell adhesion molecule (N-CAM) and L1 protein [25] or derived oligopeptides that carry the epitopes to which cells adhere through their membrane receptors (*e.g.*, integrins). Epitopes such as RGD (Arg-Gly-Asp) from fibronectin, YIGSR (Tyr-Ile-Gly-Ser-Arg) from laminin and IKVAV (Ile-Lys-Val-Ala-Val) from fibrinogen have been recognized as minimal active amino acid sequences necessary to promote cell adhesion despite the fact that they retain only 10–30% of their biological activity

as compared with the whole protein [26]. However, their higher stability against conformational change and denaturation, paired with the ability to control ligand density and orientation for more favorable ligand-receptor interactions and cell adhesion, has led them to become a cost-efficient and more durable alternative to proteins. Common adhesion and differentiation factors are listed in Table 1. Comprehensive

Table 1
Common adhesion and differentiation factors (cationic polymers and proteins or their epitopes (one-letter code)) and typical concentration ranges.

Substance (molecular weight)	Source	Reported effect or use	Typical concentration or surface coverage
Polycations			
Poly-L-lysine (PLL) (30–>300 kDa)	Synthetic	Polyamino acids facilitate the attachment of cells and proteins to solid surfaces in biological applications. [20]	0.01%
Poly-D-lysine (PDL) (30–>300 kDa)	Synthetic		0.01%
Polypropyleneimine (PPI)	Synthetic	Electropolymerization of propyleneimine or ethyleneimine monomers on fluorine-doped tin oxide (FTO) surfaces for the selective coating of metallic or semiconducting electrodes with adhesion-mediating polymer films. [25,150]	0.01%
Polyethyleneimine (PEI)	Synthetic		0.01% 0.5 μg/ml
Proteins and protein fragments			
ECM or Matrigel™	Engelbreth-Holm-Swarm murine sarcoma	Matrigel is an extract of Engelbreth-Holm-Swarm (EHS) mouse tumor. Its major components are laminin, followed by collagen IV, heparan sulfate proteoglycans, entactin and nidogen. It is used as a cell attachment factor for neurons, epithelial cells and other cell types of ectodermal and endodermal origin. It is effective for the attachment and differentiation of both normal and transformed anchorage-dependent epithelial and other cell types including neurons and oligodendrocytes [151].	6–10 μg/cm^2
Gelatin	Bovine or porcine skin	A heterogeneous mixture of water-soluble proteins of high average molecular weights is used for attachment of a variety of cell types [20], delivery vehicle for the release of bioactive molecules [152] and in the generation of scaffolds for tissue engineering applications [153].	100–200 μg/cm^2
Collagen, type I, II and IV	Bovine or porcine skin	Collagen is used in the study of growth, differentiation, migration of cell lines, and tissue morphogenesis during development [20].	6–10 μg/cm^2
Fibronectin (FN)	Bovine plasma, human plasma or human foreskin fibroblasts	Fibronectin contains several functionally and structurally distinct domains, which may bind to cell surfaces, collagen, fibrinogen or fibrin, complement, glycosaminoglycans, proteoglycans and heparin. Numerous studies have shown that fibronectin may enhance cell adhesion and spreading and affect the routes of cell migration both *in vivo* and in culture [20].	1–5 μg/cm^2
Superfibronectin	Human plasma and *Escherichia coli*	Complex of fibronectin fragment III-C and fibronectin that has greatly enhanced adhesive properties and which suppresses cell migration. Whereas cells attach to fibronectin through integrins, cell attachment to superfibronectin is mediated both by integrins and by receptors with properties distinct from those of integrins [154].	1 μg/cm^2
Fibronectin fragment III_1-C	*Escherichia coli*	[20]	0.45 μg/cm^2
Fibronectin-like protein polymer	Genetically engineered	[20]	2–10 μg/cm^2
Fibronectin proteolytic fragments	Human plasma by proteolytic enzyme digestion	Heparin and gelatin binding fragment [20]	
RGD (Arg-Gly-Asp)	Fibronectin	Minimal active amino acid sequences necessary to promote cell adhesion [26,155].	
Vitronectin (VTN)		Carries the Arg-Gly-Asp (RGD) cell recognition sequence and promotes the adhesion of various cells in culture; vitronectin binds to glycosaminoglycans [20,156].	0.1 μg/cm^2
Axonin-1		Axonin-1 strongly promotes neurite outgrowth when presented to neurons as an immobilized substratum [66,157].	80 μg/ml
Neural (N)-cadherin, neural cell adhesion molecule (N-CAM) and their respective antibodies		The adhesion on immobilized (N)-cadherin, N-CAM and their respective antibodies is concentration dependent over the whole applied range. The inferior cell–substrate adhesion at lower concentration becomes overruled by cell–cell adhesion, causing neural aggregation [25].	≤100 μg/ml
Laminin	Engelbreth-Holm-Swarm murine sarcoma basement membrane or human placenta	Laminin has active domains for collagen binding, cell adhesion, heparin binding, and neurite outgrowth fragment [158].	1–2 μg/cm^2
DEDEDYFQRYLI and DCDPGYIGSR	Laminin	Laminin peptides DEDEDYFQRYLI and DCDPGYIGSR were used to dope poly(3,4-ethylenedioxythiophene) (PEDOT) electrodeposited on platinum (Pt) electrodes for softer PEDOT films with retained neurite outgrowth bioactivity [129].	
CSRARKQAASIKVAVSADR	Laminin α1 chain, domain I, position 2091–2108	The 19-amino acid synthetic peptide CSRARKQAASIKVAVSADR-NH2 (PA22-2) from the laminin A chain sequence mediates cell-substratum adhesion and promoted neurite outgrowth [69,79].	100 μg/ml
YIGSR	Laminin	[155]	
IKVAV	Laminin	[155]	
SIKVAV	Laminin α1 chain, domain I, position 2099–2104	Cell adhesion and neurite outgrowth [155,159].	
RNIAEIIKDA	Laminin γ1 chain, domain I, position 1542–1551	Neurite outgrowth [155,159].	<0.1 mg/ml
YFQRYLI	Laminin α1 chain, domain II, position 1583–1589	Cell adhesion and neurite outgrowth [155,159].	
CDPGYIGSR	Laminin β1 chain, domain III, position 925–933	Cell adhesion [155,159].	
PDSGR	Laminin β1 chain, domain III, position 902–906	Cell adhesion [155,159].	

reviews of surface modifications for neural cell adhesion and their 2D patterning are presented in [10•,27••,28•] and in [29•,30] with an emphasis on MEA substrates. Some of the most popular techniques are exemplarily discussed in Section 5.3. Because the tissue environment is three-dimensional, there is a steady trend to extend cell culture matrices and support scaffolds to 3D as well [31•].

4. Microelectrode arrays (MEAs) — Challenges for a particular type of artificial interface

4.1. Overview on MEA types, properties and applications

Micro- or multielectrode arrays (MEAs) or multimicroelectrode plates (MMEPs) for *in vitro* electrophysiology find application in basic biological research (neuroscience, cardiology) and pharmacology [32]. Thomas, Wise and Angel, Gross and Pine pioneered MEA technology as recently reviewed [33,34]. Since then, MEAs have proven their worth in asking and answering basic neurophysiological questions underlying neural and cardiac function and pathology. Moreover, they are excellent tools for finding physiologically 'meaningful' electrical 'brain–machine' communication parameters, studying the influence of electrode topography or (bio)chemical functionalization on cellular function, understanding the biophysical events at the cell-electrode interface and characterizing the physiologically induced changes of such interface over time. They are therefore a helpful testbed for gaining a better understanding on the design requirements of neural *in vivo* probes. With the exception of nanowire and some carbon nanotube arrays, electrodes do not penetrate the cell membrane. MEAs are therefore considered 'noninvasive'.

In the field of neuroscience and neuroengineering, MEAs have firmly established their place among complementary membrane-potential sampling techniques such as patch-clamping and optical techniques including calcium imaging, potential sensitive dyes, synaptic release reporters or intrinsic signals (*e.g.*, swelling and membrane deformation due to its electromotility, changes in refractive index, changes in nerve terminal light scattering) as recently reviewed [35••,36••]. They are supplemented by emerging derivative technologies such as dielectrophoretically-accessed intracellular membrane potential measurements (DAIMM) by metal electrodes [37], metallic nanowires [38] or optical coherence tomography (OCT) [39].

Recent research explores strategies for reducing electrode impedance or enhancing the safe charge injection capacity [40••] by electrode post-modification with *e.g.*, carbon nanotubes (CNTs) [41], conductive polymers [42] or a combination of the two [43]. Additionally, there is also a steady trend in complementing classical flat, plate-like electrodes with alternative electrode designs such as single or aggregated carbon nanotube electrodes [44], nanowire field effect transistor arrays [45], graphene-based transducers [46] or a combination thereof [47]. Derivatives are light-addressable devices [48] or arrays with intercalated comb electrodes for electrical impedance spectroscopy (EIS) to study cell adhesion, cell motility and their drug-induced changes [49]. Compared to other electrophysiology techniques, MEAs are rather easy to handle. This may explain their growing popularity. Both commercial and custom-made MEAs come in a variety of designs with respect to the choice of electrode and insulator materials, electrode geometries and layout. Passive MEAs simply feature electrodes (Ø 10–120 μm, 30–500 μm pitch), contact pads and insulated leads [50•], which may come with insulator-embedded picoliter nano-cavities that render them hybrid-MEA-patch-clamp devices [51,52]. Depending on the electrode, insulation and carrier materials, they are either transparent in the visible spectrum (electrodes: indium tin oxide (ITO), fluorine-doped tin oxide (FTO), PEDOT:PSS; insulators: SiO_2, Si_3N_4, parylene-C, polyimide (PI), poly(dimethylsiloxane) (PDMS)) or opaque (electrodes: Ti, TiN, Au, Pt, Pd, Ir, iridium oxide (IrOx), polypyrrole (PPy)). Passive MEAs are complemented by active devices with on-MEA signal-conditioning electronics in complementary metal oxide semiconductor (CMOS) technology [53•] or with physically inherent amplification principles based on field-effect transistor (FET) technology [54•]. They allow for higher electrode densities up to 16,384/mm^2 due to significantly smaller electrode geometries around 16–441 μm^2 with pitches of 18–42 μm. Active CMOS and silicon-based FET devices are non-transparent in the visible spectrum, but partially transparent in the infrared. Furthermore, MEAs can carry other types of multiparametric electrochemical and optical on-chip sensors (*e.g.*, for temperature, oxygen, pH, impedance) [55].

4.2. Describing and modeling the bio-MEA interface

Unlike the stereotypic uniformity of intracellularly recorded action potentials, extracellularly recorded spikes may vary markedly in shape and polarity. They depend on the signal source, type and geometry of the cell, its developmental stage and with it the type, ratio and density of expressed (channel) proteins. Furthermore, they are regulated by activity [56•], hormones and growth factors [57] and their differential expression in pathology. Biophysically, they depend on the relative location, geometry, topography, and coating and on the resulting interfacing and electrical characteristics of the recording electrode both *in vivo* [58] and *in vitro* [59]. Predicting the efficiency of electrical stimulation of neural tissue is even more complex because it not only depends on the composition of the local microenvironment, but also on the 'edginess' and relative orientation of an electrode (and thus its E-field distribution) and on the stimulation protocol (amperostatic or potentiostatic) [40••]. This is why MEAs are ideal experimental tools for gaining a better understanding of the events at the cell-electrode interface. However, despite the large number of explanation and modeling attempts, the biophysical description and explanation of the origin and shape of extracellularly recorded signals and of the electrical stimulation efficiency of electrodes, respectively, are challenging and still under debate for metal-based electrodes [50•,60,61] as well as field effect transistors [62]. Because membrane properties (*e.g.*, fluidity, capacitance) are subject to environmental changes in their vicinity (local E-fields, temperature, pH or osmolality fluctuations, touch by migrating glia cells), signals and their recorded shapes may be prone to temporary modulation, bias or drift. This has been experimentally observed in concurrent MEA-calcium imaging experiments [63] and has been discussed theoretically for the voltage and lateral pressure dependence of the membrane capacitance in [64]. The problem can be approximately sketched and summarized as follows: extracellular electrodes sample (record) or induce (stimulate) fluctuations ΔE in the local electric field E generated by the membrane potential. In case of the existence of a thin aqueous layer between the cell and the electrode, these changes may result either from or in a transient local redistribution of ions near the electrode. If, in contrast, the electrode with its adhesion layer was in direct contact with the outer cell membrane and therefore any ionic flux between the two were to be obstructed, the electrode would sample the cytosolic potential U_{cyt} attenuated by the dielectric membrane and the adhesion layer. Not only does E for a point charge decay in first approximation at a distance r with $\Delta E \propto 1/r^2$, but also the extracellular ΔE resulting from transient cytosolic changes ΔU_{cyt} in the membrane potential U_{cyt} (with $\Delta U_{cyt} \cong 100$ mV for neurons) is very small. Therefore, electrogenic cells need to be brought into close contact with the electrodes to minimize r. However, not only the glycocalyx but also any adhesion layer acts like a spacer between the electrode surface and the cell as sketched out on the right side in Fig. 1. Depending on the visualization technique, typical thicknesses of the glycocalyx were measured around 13–17 nm up to 40 nm by transmission electron microscopy (TEM) using standard freezing protocols [65] and fluorescence interference contrast (FLIC) microscopy [66], which turn out to be around 460 nm on average in fluorescence infiltration studies [67] and as thick as 5–11 μm for endothelial and fat cells when using rapid freezing/freeze substitution (RF/FS) TEM [68]. AFM measurements revealed thicknesses of 6–28 nm for electrodeposited polymers before their exposure to

neurons [69]. Equally, a combined TEM ellipsometry study resulted in polyelectrolyte (PLL, PDL) film thicknesses below 15 nm before getting into contact with cells. However, once HEK293 cells had been cultured on these films, the resulting average cleft distances were found to be 35–40 nm for polyelectrolytes and several hundreds of nanometers for ECM proteins [70]. Interestingly adhesion turned out to be rather focal, whereas 90% of the cell membrane could be as far as 235 nm away from the sensor surface. For neurons *in vitro*, fluorescence interferometry has revealed neuron-substrate spacing of 105 nm for neurons on laminin carpets and 60 nm on fibronectin [71]. If serum supplements the cell culture medium, proteins will very likely interact with and deposit on the adhesion layer, thereby further thickening the cushion between cell and electrode by an undefined amount. Taking the above mentioned $1/r^2$ dependency of the E-field and approximating the bulk extracellular space to be grounded ($U_{ECM} = 0$ V), a sample calculation would result in an E-field decay over the cell membrane (with thickness $d \cong 10$ nm) and the adhesion film by a factor of 144 to 256 for thin polyelectrolyte adhesion mediators in direct contact with the cell. In contrast, attenuation factors of 400 to several ten thousands for thick protein adhesion layers will very likely prevent the electrode from directly sensing the intracellular potential swing. If, in addition, the glycocalyx together with the adhesion layer are gel-like and allow for the unobstructed passage of ions (like in a loose-patch configuration in patch clamping) [67], the transient field-generating local ionic imbalance or asymmetry may be balanced out too quickly from ionic influx from bulk solution to drive a detectable capacitively induced charge shift in the electrode material. The situation can be compared to a simple resistive voltage splitter. Signals will simply dissipate along the path of highest electrical conductivity towards ground. This affects in particular small recording electrodes with impedances orders of magnitude higher than that of the cell culture medium or its seal resistance at the membrane-electrode gap. However, over time, this leakage pathway can be closed by cell debris or, more likely and effectively, by the 'insulating' cell membranes of proliferating glial cells.

For electrical stimulation of neural activity, MEA users have to address another problem, the alteration of the local chemical environment by electrochemically generated side-products. With Ohm's law ($U = R \cdot I$), the voltage U is free to float in amperostatic stimulation protocols. This may lead to Faradaic currents beyond the safe charge-injection capacity of the electrode [40••]. In this instance, electrons will cross the electrode interface into the solution. However, electrons, not being soluble in aqueous solutions, will immediately involve and be consumed in chemical redox-reactions. If reaction kinetics are slow with respect to stimulation pulse widths, biphasic current pulses of opposite polarity may reverse and thus attenuate the formation of uncontrollable and undesirable side products. However, in most cases these reactions are partially irreversible. The accumulation of side products or gas microbubbles (upon splitting water at voltages around 1.2 V, depending on electrode material (overpotential) and environment) will alter electrode characteristics over time.

The existence of many parasitic signal degradation pathways may actually explain the recent success of nanostructured microelectrodes with (arbitrarily) protruding nanotubes [41•] and that of nanowire electrode devices and nanoscale transistors [72], respectively. The protein coating on these nanotextures is very likely inhomogeneous and thus allows for conductive particles penetrating the adhesion-mediating film, thereby getting in closer (multipoint) contact to the cell membrane. Signal amplitudes are boosted by a factor of 10 to 50 from usually tens of microvolts to millivolts. Apart from increasing the overall capacitance by enlarging the real surface by a factor of 100–1000 with respect to the geometrical surface area, structuring or roughening electrodes by electrochemical deposition (or other techniques) may have a similar effect by creating very fine and irregular, sometimes quasi-fractal surface topographies or porosities [73,74]. Graham et al. demonstrated with NG108-15 mouse neuroblastoma/rat glioma hybrid cells that the porosity of biocompatible porous alumina (Al_2O_3) had no aversive effect on cell vitality, but improved cell adhesion [75]. Equally, nano-porous silicon (pSi), which can also be used for drug delivery, induced increased extension of neurites from PC12 pheochromocytoma cells compared to smooth silicon surfaces [76]. The cell-electrode gap can be narrowed by various other strategies. Signal amplitudes were successfully boosted by allowing the cell membrane to engulf epitope-decorated 1.4 μm high gold mushroom-shaped microelectrodes (gMμEs) in a phagocytosis-like process, thereby tightening the seal around the recording site at its head (Ø ~1 μm) [77,78•] (Fig. 3-3). Van Meerbergen et al. suggested the phagocytosis of CRGD- and laminin-epitope (PA22)-functionalized gold microneedles [79]. Robinson et al. recently demonstrated that the cytosolic potential could indeed be probed with tips of 3 μm-long silicon vertical nanowire (Ø 150 nm) electrode arrays (VNEAs) that penetrated the cell membrane upon short voltage pulses [80]. Similarly, glass nanotubes on nanowire field-effect transistors, whose performance does not depend on impedance, may penetrate the cell membrane and thus directly sample the intracellular transmembrane potential [81]. These electrodes, nanotubes or nanowire stalks can furthermore be decorated by phospholipids [82]. Upon interaction with the cell and the careful perforation of its membrane, the lipids tend to fuse with the cell membrane, thereby forming a tight seal. Currently, these technologies as reviewed in [78•,83•] are lab prototypes and not yet commercially available.

These considerations apply only to non-myelinated cell processes and somata unobstructed by glial cells. A separate debate on the role and problematic nature of glial cells adds uncertainty and difficulty to this discussion on how extracellularly recorded signals can be interpreted and faithfully modeled. Glia cells play a vital part in neural function and signal propagation. Yet, in MEA electrophysiology, there is still uncertainty about the tendency of glial cells sliding between the neuron and the electrode. Glia may thereby lift and electrically isolate the neuron from the electrode and attenuate if not abolish recordable signals [84], which is a serious issue for *in vivo* MEAs [85]. Glia proliferation can be slowed down during the first few days to weeks by using serum-free media or adding antimitotic or antimetabolic agents such as 5-fluoro-2′-deoxyuridine or arabinofuranosyl cytidine (Ara-C) to the medium. However, by excluding glia contribution one runs the risk of distorting biological functions and, in consequence, the significance of recorded and induced signals. Similarly, while signals may be more easily recorded from unmyelinated axons, information transfer in unmyelinated networks will very likely have significantly different spatio-temporal characteristics. Action potentials may be exhausted after shorter distances for lack of the natural 'signal refreshing mechanism' at internodes. Equally likely, they will travel more slowly due to the lack of the salutatory conduction mechanism.

5. Cell adhesion and cell confinement — Common necessities and particular needs for MEA electrophysiology

The interfacial chemistry and physics at bio-hardware interfaces have become one of the cornerstones in bioanalysis and tissue engineering. The understanding of the regulatory role of chemical and topological interface features determines the quality and durability of a device-tissue symbiosis [86•,87•]. Growing cells on MEAs is just one particular application in this context. Therefore, substrate treatment needs and concepts are similar to those found in other application fields. By placing physico-chemical cues, neuronal fate, cell and axon migration as well as cellular differentiation can be investigated and steered [88]. Because several excellent reviews cover this topic [10•,27••,28] with particular focus on MEAs [29•,30], this section restricts itself to a general overview on surface modification strategies for cell attachment and alignment. They include topographic modifications and the spatial patterning of cell adhesive zones.

Regarding MEAs, the main goal is to bring a selected number of neurons into close vicinity to the electrodes. On passive MEAs, electrodes consume less than 5% of the surface area. Therefore, chances

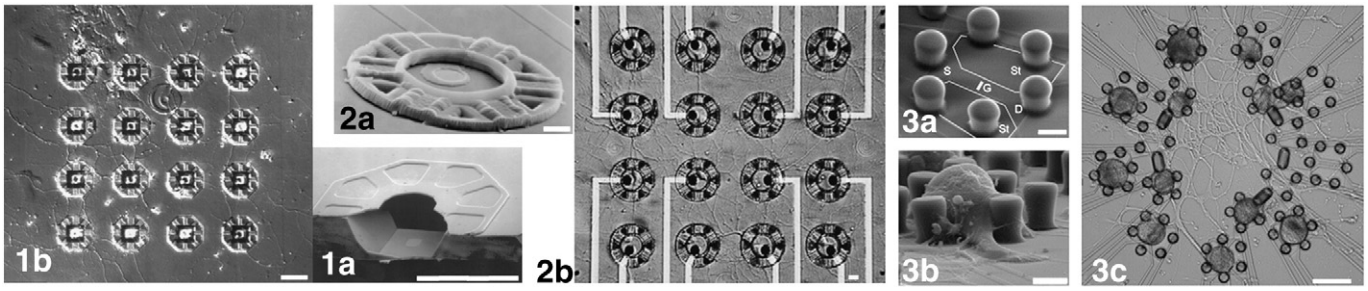

Fig. 2. Neurowell in silicon (1) [93] and parylene neurocage (2) design on passive MEAs [97], and polyimide picket fences on a field-effect transistor MEA (3) [94]. 1a The neurowell featured a silicon nitride canopy with radially raised bars as tunnels through which neural processes could grow. A central 10 μm diameter hole allowed the insertion of a single neuron. The well walls exposed the silicon <111> planes formed by an anisotropic etch. The floor of the well was a suspended film of silicon nitride with a 6 μm square gold electrode. 1b A 4 · 4 neurowell MEA with a hippocampal network after 8 days in culture (left). Scale bars are 20 μm. 2a SEM of a 4 μm high parylene neurocage with a central chimney atop a passive microelectrode. Low-stress silicon nitride insulated the leads. 2b Rat hippocampal culture on a 4 · 4 neurocage MEA after 10 days *in vitro* with entrapped somata and processes growing through the tunnels. Scale bars are 10 μm. 3a Polyimide fence with five pickets around stimulator wings (St) and recording transistor (S source, D drain, G gate) with 3b a neuron from the A cluster of the pedal ganglia in *Lymnaea stagnalis* after three days in culture (scale bars are 20 μm) and 3c interconnected neurons after two days in culture. Scale bar is 100 μm. Adapted with permission from the copyright owners.

are high that neurons, statistically seeded at low to medium densities (100–10,000 cells/mm^2), may never settle their somata or neurites on or sufficiently near the recording or stimulation electrodes. Undifferentiated neurons are initially very motile in search of adhesion cues. Once found, they immobilize and activate their differentiation program. Only their processes will explore the surroundings and adjust their cytoskeletal organization to changes in their vicinity (because differentiating and maturing primary (non-tumor-line) neurons do not divide). Therefore, most strategies focus on seeding neurons as closely as possible to the electrode and guide neurites along 'highways' to adjacent electrodes. While there may not necessarily be any biological significance in the latter, it helps in imaging, identifying and tracing processes and signal flow from source to target. It was also found to enhance neural activity [89]. Finally, it facilitates the manipulation of neurites *e.g.*, by optical tweezers [90] or laser microdissection [91], the probing of the mechano-biology of neural function and the study of neural regeneration [92].

5.1. Physical confinement and structural cues

Four types of physico-structural confinements can be distinguished. The first confines neurons or their processes to certain locations in a bottom–up approach, either by microwells etched in bulk silicon [93] (Fig. 2-1), polyimide picket fences [94] (Fig. 2-3), SU-8 microwells [95], stepwise photo-thermally etched channels in agarose [96], parylene neurowells [33,97] (Fig. 2-2) or by protruding anchors [78•,98,99] (Fig. 3-2,3). In both cases, the goal is to reduce migration tendency and increase the soma-electrode contact.

The second type of physical cue aims at guiding processes into predefined directions *e.g.*, by μ-fluidic polymer [100•,101] or hydrogel (alginate) [102] channels, or nanowire fences [103]. Microchannels not only guide processes, but may also impose a preferred signal-propagation direction [104]. They also create an artificial myelin sheath-like seal around axons, thereby notably increasing the signal-to-noise ratio from usually 5–10 to >100 [101,105]. In addition, diffusion has been shown to be greatly attenuated in channels with small cross-sections [106], which not only allows the separation of neural compartments, but also stabilizes the local signaling factor microenvironment. Moreover, if microchannel devices are made from gas-permeable materials (*e.g.*, PDMS) and self-contained with sufficiently thin walls, cells may benefit from increased oxygen supply [107]. While in some cases confinements are an integral part of a MEA [30], they are usually added as a supplementary feature in a post-processing step. For line- or stripe-electrode MEAs [101,108], microchannel devices can be placed on the substrate without the need for their precise alignment. In all other cases, their accurate positioning with respect to individual electrodes is

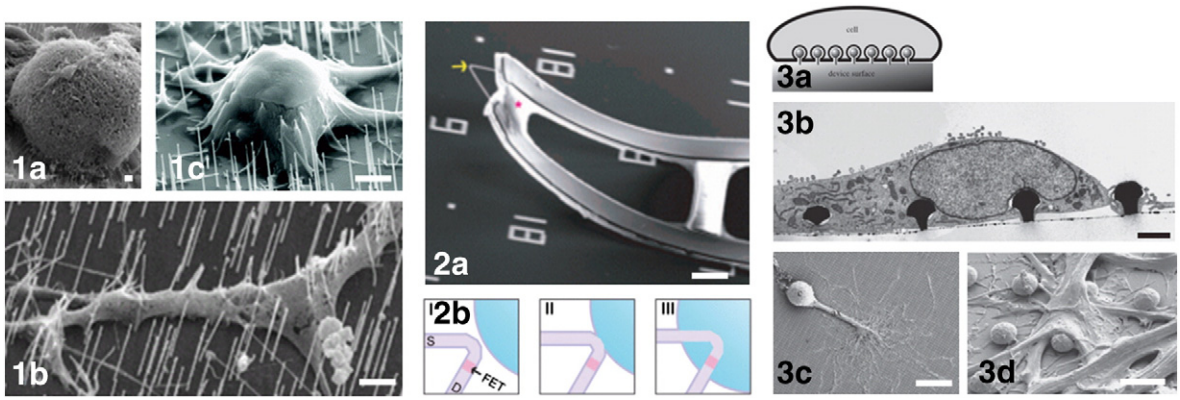

Fig. 3. 1 SEM-images showing interaction between nanowires and cells and cell processes. 1a Neural cell body on nanowires surfaces. 1b Process spreading over the bulk substrate, apparently engulfing nanowires encountered along its path [99]. 1c Scanning electron microscopy (SEM) image of mouse embryonic stem (mES) stem cell on a nanowire array substrate penetrated with silicon nanowires. The diameter and the length of the nanowires were 90 nm and 6 μm, respectively [98]. Scale bars are 1 μm. 2a SEM of a 3D kinked nanowire probe. The yellow arrow and pink star mark the nanoscale FET and SU-8 photoresist, respectively. Scale bar is 5 μm. 2b I–III Schematics of nanowire probe entrance into a cell. Dark purple, light purple, pink, and blue colors denote the phospholipid bilayers, heavily doped nanowire segments, active sensor segment, and cytosol, respectively [160]. 3a Concept and 3b transmission electron microscopic (TEM) image of gold spines engulfed by a 3T3 cell. Scale bar is 2 μm. 3c and 3d SEM images of a neuron isolated from *Aplysia* grown on gold-spine matrices. Scale bars are 100 μm and 2 μm, respectively [77]. Adapted with permission from the copyright owners.

required. The most popular material for the production of microchannel devices is poly(dimethylsiloxane) (PDMS). It allows the rapid replica-molding production and reversible device placement onto the substrate. Microchannels can therefore be removed at any desired time *i.e.* to facilitate cell-staining or imaging. Being an established technology in tissue-engineering [31•,109], the advent of 3D additive manufacturing is expected to play an increasing role in the rapid and easy creation of physical confinements on plane and pre-structured devices.

The third type of physical cue exploits textural and structural properties of a substrate after observing that the behavior of cells on surfaces with certain geometric profiles like edges, grooves [110], gratings, pillars or holes (10 nm to several μm) or other features such as stiffness [110] or pattern anisotropy [111] is significantly different from cell behavior on perfectly smooth surfaces. Production processes and effects of textural and structural features on protein adsorption and cell behavior have therefore been subject of numerous reviews [12•,112•]. Only a subset of these techniques has been tested on neurons and even fewer have been applied to MEAs.

The fourth type of physical confinement is of temporary nature and aims at the patterned placement of neurons by means of pneumatic anchoring with through-chip holes [113], dielectrophoretic trapping through a set of auxiliary electrodes [114,115], optical tweezers [116], optical image-driven dielectrophoresis [117], *in situ* barrier formation in BSA [118], microfluidics [119], or inkjet printing [120]. A recent review outlines the emerging use of inkjet printing in tissue engineering and biofabrication applications [121].

In a top–down strategy, cellular assemblies or networks can be structured by (UV) [92] or thermal (NIR, $\lambda \geq 800$ nm) laser-ablation [122]. While these two methods are destructive, Ehrlicher et al. showed that neural growth can also be directed by the gradient force of an NIR laser (Ø 2–16 μm, power 20–120 mW, $\lambda = 800$ nm) by biasing the actin polymerization-driven lamellipodial extension at the growth cone [123].

5.2. (Bio)chemical cues

Recently, materials like graphene have been screened not only for their suitability as electrode material, but also for promoting neural sprouting and neurite extension [124] without any additional supporting glial layer or protein coating [125]. Likewise, carbon nanotubes (CNTs) were found to be equally good adhesion mediators (without further chemical modification) and signal boosters [41•]. Although to date there is no direct comparison with other conductive materials, these enhancements may not exclusively be rooted in the conductivity of the material itself, but partially result from their particular chemistry and geometry.

It is a common procedure to expose cell cultureware and MEAs to oxygen plasma, corona discharge or the flame of a propane torch [84] to render most insulators including glass and polystyrene (PS) as well as electrode materials more hydrophilic. In some cases, this treatment seems to sufficiently support cell attachment without any further chemical substrate modification. While this may come as a surprise at first (because any of the abovementioned treatments creates a mostly negatively charged interface), it is likely that adhesion is indirectly mediated by a metalayer of proteins in serum-containing media. Table 1 lists the most commonly used adhesion mediators in MEA electrophysiology studies. They can be transferred to and patterned on the (MEA) substrate in various ways as summarized below and reviewed in [29•].

With the exception of all-diamond MEAs [126] and some FET MEAs that carry the same dielectric layer for the gate as used for device insulation, the different types and classes of materials for electrodes and insulators make their interfaces chemically inhomogeneous. Due to different interaction forces, this may affect deposition efficiency and wear resistance of adhesion mediators on the different kinds of materials. Moreover, in most cases, electrodes are intentionally or for production-related reasons slightly recessed with respect to the insulation layer. Consequently, some of the (protein) deposition techniques (*e.g.*, soft lithography) that depend on substrate planarity will transfer unequal amounts of their polymer or protein ink to different areas.

5.3. Common patterning techniques of adhesive or anti-adhesive deposits

There are several ways to apply and predictably pattern adhesion-mediating films on artificial cell culturing, tissue culturing, or implant surfaces. They may be preceded by micro- or nanostructuring processes of the substrate. General pattern generation approaches are reviewed in [10•,27••,28•] and in [29•,30] with an emphasis on MEA substrates. Some representative techniques are summarized in the following paragraphs and graphically shown in Fig. 4.

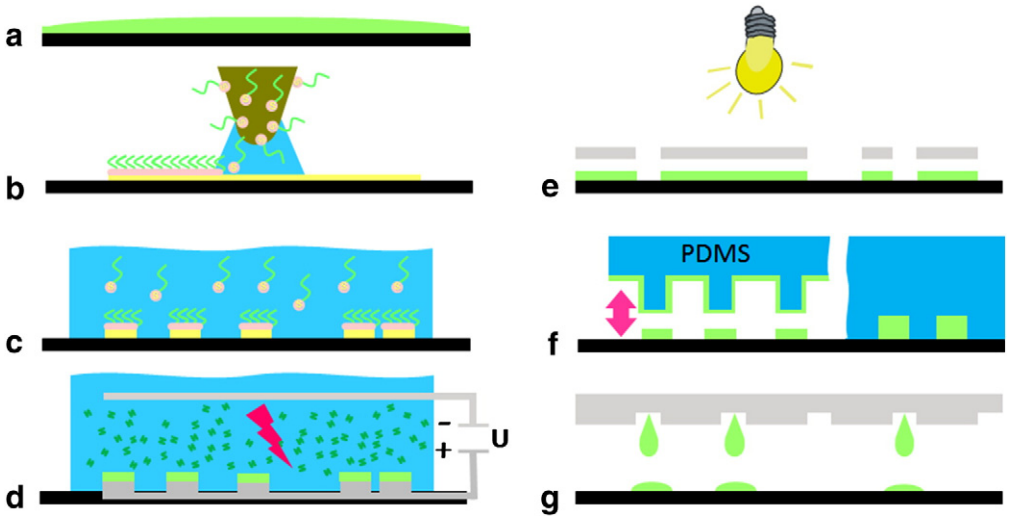

Fig. 4. Comparative overview of different popular substrate patterning techniques with chemical adhesion and guidance cues or growth factors (green). a Global coating; b dip-pen nanolithography (DPN) or scanning probe lithography (SPL) of adhesion mediators that carry a sulfur anchor (*e.g.*, cysteine group) to form self-assembling monolayers (SAMs) on (patterned) gold substrates or electrodes; c SAM formation on patterned gold substrates; d electrochemical deposition of electropolymerizable bio-functional monomers or of adhesion mediators with electropolymerizable anchor group; e photolithographic ablation/desorption of adhesion mediator from illuminated substrate zones; f soft lithographic stamping of adhesion mediator ink onto substrate (left) or microfluidic incubation of surface with adhesion mediator solution (right); g inkjet deposition.

The easiest and most common technique is to globally coat any substrate with common adhesion mediators such as polylysine, fibronectin, laminin, or anti-adhesive compounds (Fig. 4a). A solution is distributed on the substrate surface. After incubation (minutes to hours) or drying, the substrate is rinsed thoroughly for the removal of non-adsorbed excess material. Higher concentrations are not always better, particularly for proteins. It seems that functional efficiency follows a hill-shaped trend with an optimal surface density around 1–10 μg/cm^2.

If electrodes or surface sections expose gold, thiol-derivatives of adhesion mediators can be applied and patterned onto them with the help of the tip of an atomic force microscope (AFM) in dip-pen nanolithography (DPN) or scanning probe lithography (SPL) (Fig. 4b). The thiol-groups will form covalent bonds with the gold. Depending on its three-dimensional structure, the adhesion mediator might self-assemble on the gold to result in patches or dense carpets of so-called self-assembling monolayers (SAMs) [127]. Like bristles of a brush, they align automatically to give a homogeneous and highly ordered closed carpet [128]. The AFM tip can also be used in an inverse fashion, *e.g.*, for scratching a local lane into a homogeneous coat to expose the substrate or other layers below [9•].

Alternatively, if only the electrodes are made of gold, this strategy will allow the dipping of the substrate into a solution of the thiol-modified adhesion mediator. As a result, the thiol anchor will covalently link the adhesion mediator to the gold to form a SAM being restricted to the electrodes only (Fig. 4c).

Because electrodes in passive and some active devices are electrically accessible and addressable by electrochemical deposition and characterization techniques (*e.g.*, cyclovoltammetry (CV), chronoamperometry), metals (Pt, Au, TiN, IrOx) or conductive polymers (PPy, PEDOT:PSS) with entrapped adhesion mediators [129] can be deposited on them (Fig. 4d). An electrochemical co-deposition of conductors and biomolecules has the advantage of not only enhancing the impedance characteristics of an electrode, but also intercalate bioactive substances with the often highly porous deposits. They may not only promote cell adhesion, but also act as electro-actuatable reservoirs for the controlled release of neurotransmitters, signaling and growth factors or drugs as reviewed in [130].

If the adhesion mediator itself is carrying an electrochemically active anchor group (*e.g.*, phenol, pyrrole, aniline, dopamine), it can be electrochemically deposited onto the electrode or any electroconductive substrate. The anchor groups will electropolymerize, thereby forming a variably homogenous polymer film depending on the electrical characteristics (insulating or conductive) of the generated polymer and the presence and type of deposition adjuvants or chelating agents. Because most electrodes are not perfectly flat, the abovementioned film will be entrapped by the rough surface and be mechanically anchored in grooves. Physisorption and/or chemisorption will support the anchoring. The side chains of such film will then be responsible for mediating the cell adhesion for attracting and anchoring neurons onto the electrodes [69,131]. Electroswitchable anchors furthermore allow for the dynamic and selective release of adherent cells [132].

If pre-patterned substrates are not available, or the gold-coated electrodes or substrates are not suitable for the desired application, the adhesion mediator can be patterned directly onto the substrate in so-called soft lithography by means of a micro-patterned polymer stamp, *e.g.*, made from poly(dimethylsiloxane) (PDMS) [133••,134•] (Fig. 4f left). Depending on stamp treatment and deposition technique, this approach allows for the subsequent use of the same or different stamps with different patterns and/or coatings to apply complex adhesion mediating patterns onto the substrate. Theoretically, the ink dispenser could be structured instead (as in pad printing). However, if the ink film is thin and colorless, relative alignment between device and stamp would be difficult without other alignment marks or auto-alignment aids (such as frames on the substrate). Gradients can be created through spatial anisotropy [135]. The contrast between adhesive and anti-adhesive areas on the substrate can be enhanced by stamping anti-adhesive compounds into the remaining spaces or by stamping adhesion mediators onto a non-permissive meta-layer (*e.g.*, 3-glycidoxypropyl trimethoxysilane (3-GPS)) [136]. A variation is capillary force lithography (CFL), where capillary forces draw a thin solution or gel film of anti-adhesive material (*e.g.*, hyaluronic acid (HA), polyethylene glycols (PEGs)) into the interspace of the stamp-substrate contact of a loosely seated, quasi-floating stamp. The mechanism feeds from through-holes in the stamp, which locally dewet the substrate in these areas. The exposed substrate in these through-holes can then be coated by an adhesion mediator [137]. Such 'stealth' or 'non-fouling' ultra-low attachment areas will maintain cells in a suspended, unattached state, thereby preventing them from attachment-mediated division and differentiation, and reducing the binding of attachment and serum proteins. Transferring the adhesion-mediator ink from a stamp onto the substrate is an art in itself. Its success seems not only to depend on the stamp material (usually silicone), its pre-treatment (*e.g.*, curing temperature and time, elution of uncured oligomers, silanization, hydrophilicity, contact time and pressure), but also on the ambient conditions such as relative humidity and temperature. Keeping the stamp at low temperature (*e.g.*, in a refrigerator) or breathing onto it right before stamp deposition will ensure sufficient formation of water condensate to promote ink transfer onto a substrate [138]. However, the breathing strategy will probably compromise sterility. Alternatively, roughening stamp and substrate at the nanometer scale (<20 nm) have been found to improve ink transfer two- to twenty-fold [139].

Said stamp can also be designed as a microfluidic structure and then be used inversely (Fig. 4f right). After placing it onto the substrate, the microchannels are filled with the surface-modifying compound (*e.g.*, polyelectrolyte [140] or proteins [119]) and replaced by water or medium after sufficient incubation. If the microfluidic device is kept on the substrate, this approach avoids the need for blocking agents on non-coated substrate areas. Alternatively, the microchannels can be lifted off the device after patterning. Also microfluidic deposition can be repeated sequentially for generating complex patterns [141].

For planar and non-planar substrate geometries alike, adhesion mediators can be printed simultaneously in patterns by means of an inkjet printer or micro/nanodrop deposition device [142] (Fig. 4g). While most commercial printers feature sufficiently high printing resolutions down to several tens of micrometers, their ink ejection mechanism may differ (thermal *versus* piezo). It is not clear whether thermal ejection will lead to a denaturing or otherwise non-controllable change in bioink chemistry.

A less common method with high alignment precision and spatial resolution is the application of photoresist as a temporary substrate masking layer, its exposure through a photolithography mask to define patterns, the removal (development) of non-cured photoresist after crosslinking and the soaking of the exposed substrate surface in a solution of adhesion mediators for some time. A subsequent solvent exposure will dissolve and wash away the cured photoresist, thereby uncovering the previously masked areas without adhesive cues [143] (Fig. 4e). The process flow can be inverted too. In that case, the adhesion mediator needs protection against contamination by the photoresist, *e.g.*, with the help of an intermediate sucrose layer [144]. Alternatively, adhesion layers can be structured by UV (<200 nm) laser or excimer lamp ablation either through a photolithography mask [145] or by laser-scanning desorption lithography (LSL) with features ranging from 460 nm to 100 μm, topographies below 17 nm, and both stepwise or smooth ligand surface density gradients [146]. Contrast between adhesive and non-permissive areas can be enhanced by adding a proteinophobic background, *e.g.*, with adsorbed layers of poly(ethylene glycol) (PEG) [147] or polyethylenoxide–polypropylenoxide (PEO–PPO) blockcopolymers (*e.g.*, Synperonics F108 and F127) [148] before patterning the adhesion mediator on top of it. If resolutions above 100 μm are acceptable, patterns can be dynamically generated in photocrosslinkable hydrogels using simple optics and a digital micromirror (DMM) projection array [149].

6. Concluding discussion and remarks

This overview focused on *in vitro* MEA surface modification strategies for enhancing both the signal-to-noise ratio and the electrical stimulation efficacy as well as controlling network architecture. While these are desirable aspects for *in vivo* MEAs as well, strategies may differ from those *in vitro*. The main reason is a more complex biochemical *in vivo* environment, which also involves the body's immune response. In addition, detached surface modifiers may accumulate more easily *in vivo* contributing to inflammation or device rejection. Even more importantly, the *in vivo* insertion of MEAs causes damage, which requires the consideration of additional strategies and measures to attenuate inflammatory responses and deliver growth factors in support of a stable tissue integration.

Given the variety of materials and associated substrate surface characteristics for MEA electrode and insulation materials, the deposition efficiency and functionality of an adhesion mediating film may vary considerably. As an example, PEDOT:PSS coatings from the very same aqueous dispersion show different conductivity on different substrates such as glass, plastic Petri dishes or PDMS. Differences can reach one order of magnitude (unpublished data). Although the general working principle of a substance and its deposition protocol does not need to be questioned, the observation exemplifies the difficulty of predicting the functional outcome of a certain biofunctional coating, which may work in a particular experimental and material context, but may be sub-optimal or even fail in another. Therefore, quite often a standard protocol has to be adjusted and fine-tuned for a particular situation.

This overview presented only a subset of adhesion chemistry and cell guiding strategies, which have been tested mostly in non-MEA related contexts, but may be applicable to MEA substrates as well. However, because cell adhesion and patterning strategies come in hundreds of variations, it is no trivial task to get a holistic overview and make an educated decision on their suitability and usefulness for MEA electrophysiology. Yet, the MEA community will without doubt benefit from the large variety of possibilities and permutations of combining and structuring adhesion mediators as 2D films or 3D matrices and of their enhancement by auxiliary functionalities (*e.g.*, loading with growth factors, drugs, nanoparticles) towards more tissue-analog *in vitro* models.

Acknowledgments

Many thanks to Virginia Giannelli for her critical proofreading of the final manuscript. This work was supported by intramural funds of the Italian Institute of Technology Foundation.

References and recommended reading[•,••]

[1] Stüeken EE, Anderson RE, Bowman JS, Brazelton WJ, Colangelo-Lillis J, Goldman AD, et al. Did life originate from a global chemical reactor? Geobiology 2013;11:101–26.
[2] Gumbiner BM. Cell adhesion: the molecular basis of tissue architecture and morphogenesis. Cell 1996;84:345–57.
[3] Wolfenson H, Lavelin I, Geiger B. Dynamic regulation of the structure and functions of integrin adhesions. Dev Cell 2013;24:447–58.
[4] Barros CS, Franco SJ, Müller U. Extracellular matrix: functions in the nervous system. Cold Spring Harb Perspect Biol 2011;3.
[5] Mecham RP. Overview of extracellular matrix. Curr Protoc Cell Biol 2012;57:10.1.1–10.1.16.
[6] Karmiol S, Manaster E, Ryan J. Attachment and matrix factors. Biofiles (Sigma-Aldrich) 2008:3.
[7] El-Ali J, Sorger PK, Jensen KF. Cells on chips. Nature 2006;442:403–11.
[8] Chan G, Mooney DJ. New materials for tissue engineering: towards greater control over the biological response. Trends Biotechnol 2008;26:382–92.
[9] Koegler P, Clayton A, Thissen H, Santos GN, Kingshott P. The influence of nanostructured materials on biointerfacial interactions. Adv Drug Deliv Rev 2012;64:1820–39.
[10] Ross AM, Lahann J. Surface engineering the cellular microenvironment via patterning and gradients. J Polym Sci, Part B: Polym Phys 2013;51:775–94.
[11] Hoffman BD, Grashoff C, Schwartz MA. Dynamic molecular processes mediate cellular mechanotransduction. Nature 2011;475:316–23.
[12] Ross AM, Jiang Z, Bastmeyer M, Lahann J. Physical aspects of cell culture substrates: topography, roughness, and elasticity. Small 2012;8:336–55.
[13] Cranford SW, de Boer J, van Blitterswijk C, Buehler MJ. Materiomics: an -omics approach to biomaterials research. Adv Mater 2013;25:802–24.
[14] Lensen MC, Schulte VA, Salber J, Diez M, Menges F, Möller M. Cellular responses to novel, micropatterned biomaterials. Pure Appl Chem 2008;80:2479–87.
[15] Koch K, Bhushan B, Barthlott W. Multifunctional plant surfaces and smart materials. In: Bhushan B, editor. Springer handbook of nanotechnology. Berlin Heidelberg: Springer; 2010. p. 1399–436.
[16] Liu K, Tian Y, Jiang L. Bio-inspired superoleophobic and smart materials: design, fabrication, and application. Prog Mater Sci 2013;58:503–64.
[17] Fenoglio I, Fubini B, Ghibaudi EM, Turci F. Multiple aspects of the interaction of biomacromolecules with inorganic surfaces. Adv Drug Deliv Rev 2011;63:1186–209.
[18] Latour RA. Biomaterials: protein-surface interactions. Encyclopedia of Biomaterials and Biomedical Engineering. Taylor & Francis; 2013 1–15.
[19] Zhang P-C, Keleshian AM, Sachs F. Voltage-induced membrane movement. Nature 2001;413:428–32.
[20] Sitterley G. Attachment and matrix factors. Biofiles (Sigma-Aldrich) 2008;3:1–28.
[21] De Smedt SC, Demeester J, Hennink WE. Cationic polymer based gene delivery systems. Pharm Res 2000;17:113–26.
[22] Mayhew E, Harlos JP, Juliano RL. The effect of polycations on cell membrane stability and transport processes. J Membr Biol 1973;14:213–28.
[23] Fischer D, Li Y, Ahlemeyer B, Krieglstein J, Kissel T. In vitro cytotoxicity testing of polycations: influence of polymer structure on cell viability and hemolysis. Biomaterials 2003;24:1121–31.
[24] Richert L, Arntz Y, Schaaf P, Voegel JC, Picart C. pH dependent growth of poly(l-lysine)/poly(l-glutamic) acid multilayer films and their cell adhesion properties. Surf Sci 2004;570:13–29.
[25] Wiertz RWF, Marani E, Rutten WLC. Neural cell–cell and cell-substrate adhesion through N-cadherin, N-CAM and L1. J Neural Eng 2011;8.
[26] Ruoslahti E. RGD and other recognition sequences for integrins. Annu Rev Cell Dev Biol 1996;12:697–715.
[27] Khan S, Newaz G. A comprehensive review of surface modification for neural cell adhesion and patterning. J Biomed Mater Res A 2010;93A:1209–24.
[28] Meiners F, Plettenberg I, Witt J, Vaske B, Lesch A, Brand I, et al. Local control of protein binding and cell adhesion by patterned organic thin films. Anal Bioanal Chem 2013;405:3673–91.
[29] Chang J, Wheeler B. Pattern technologies for structuring neuronal networks on MEAs. In: Taketani M, Baudry M, editors. Advances in network electrophysiology. US: Springer; 2006. p. 153–89.
[30] Wheeler BC, Brewer GJ. Designing neural networks in culture. Proc IEEE 2010;98:398–406.
[31] Zorlutuna P, Annabi N, Camci-Unal G, Nikkhah M, Cha JM, Nichol JW, et al. Microfabricated biomaterials for engineering 3D tissues. Adv Mater 2012;24:1782–804.
[32] Johnstone AF, Gross GW, Weiss DG, Schroeder OH, Gramowski A, Shafer TJ. Microelectrode arrays: a physiologically based neurotoxicity testing platform for the 21st century. Neurotoxicology 2010;31:331–50.
[33] Pine J. Neurochip. Scholarpedia 2008;3:7766.
[34] Gross GW. Multielectrode arrays. 2011;6:5749.
[35] Scanziani M, Hausser M. Electrophysiology in the age of light. Nature 2009;461:930–9.
[36] Peterka DS, Takahashi H, Yuste R. Imaging voltage in neurons. Neuron 2011;69:9–21.
[37] Terpitz U, Sukhorukov VL, Zimmermann D. Prototype for automatable, dielectrophoretically-accessed intracellular membrane—potential measurements by metal electrodes. Assay Drug Dev Technol 2013;11(1):9–16.
[38] Angle MR, Schaefer AT. Neuronal recordings with solid-conductor intracellular nanoelectrodes (SCINEs). PLoS One 2012;7:e43194.
[39] Akkin T, Landowne D, Sivaprakasam A. Optical coherence tomography phase measurement of transient changes in squid giant axons during activity. J Membr Biol 2009;231:35–46.
[40] Cogan SF. Neural stimulation and recording electrodes. Annu Rev Biomed Eng 2008;10:275–309.
[41] Bareket-Keren L, Hanein Y. Carbon nanotube-based multi electrode arrays for neuronal interfacing: progress and prospects. Front Neural Circuits 2012;6:122.
[42] Green RA, Lovell NH, Wallace GG, Poole-Warren LA. Conducting polymers for neural interfaces: challenges in developing an effective long-term implant. Biomaterials 2008;29:3393–9.
[43] Gerwig R, Fuchsberger K, Schroeppel B, Link GS, Heusel G, Kraushaar U, et al. PEDOT-CNT composite microelectrodes for recording and electrostimulation applications: fabrication, morphology and electrical properties. Front Neuroeng 2012;5.
[44] Wang K, Fishman HA, Dai H, Harris JS. Neural stimulation with a carbon nanotube microelectrode array. Nano Lett 2006;6:2043–8.
[45] Yang L, Li Y, Fang Y. Nanodevices for cellular interfaces and electrophysiological recording. Adv Mater 2013;25(28):3881–7.
[46] Hess LH, Seifert M, Garrido JA. Graphene transistors for bioelectronics (arXiv preprint arXiv:13021418) ; 2013 .
[47] Lee SK, Kim H, Shim BS. Graphene: an emerging material for biological tissue engineering. Carbon Lett 2013;14:63–75.
[48] Stein B, George M, Gaub HE, Parak WJ. Extracellular measurements of averaged ionic currents with the light-addressable potentiometric sensor (LAPS). Sensors Actuators B: Chem 2004;98:299–304.

• Of special interest.
•• Of outstanding interest.

[49] Wegener J, Keese CR, Giaever I. Electric cell-substrate impedance sensing (ECIS) as a noninvasive means to monitor the kinetics of cell spreading to artificial surfaces. Exp Cell Res 2000;259:158–66.
[50] Rutten WLC. Selective electrical interfaces with the nervous system. Annu Rev Biomed Eng 2002;4:407–52.
[51] Baaken G, Sondermann M, Schlemmer C, Ruhe J, Behrends JC. Planar microelectrode-cavity array for high-resolution and parallel electrical recording of membrane ionic currents. Lab Chip 2008;8:938–44.
[52] Hofmann B, Katelhon E, Schottdorf M, Offenhausser A, Wolfrum B. Nanocavity electrode array for recording from electrogenic cells. Lab Chip 2011;11:1054–8.
[53] Hierlemann A, Frey U, Hafizovic S, Heer F. Growing cells atop microelectronic chips: interfacing electrogenic cells in vitro with CMOS-based microelectrode arrays. Proc IEEE 2011;99:252–84.
[54] Poghossian A, Ingebrandt S, Offenhausser A, Schoning MJ. Field-effect devices for detecting cellular signals. Semin Cell Dev Biol 2009;20:41–8.
[55] Ehret R, Baumann W, Brischwein M, Lehmann M, Henning T, Freund I, et al. Multiparametric microsensor chips for screening applications. Fresenius J Anal Chem 2001;369:30–5.
[56] Laufer R, Changeux J-P. Activity-dependent regulation of gene expression in muscle and neuronal cells. Mol Neurobiol 1989;3:1–53.
[57] Chew L-J, Gallo V. Regulation of ion channel expression in neural cells by hormones and growth factors. Mol Neurobiol 1998;18:175–225.
[58] Humphrey D, Schmidt E. Extracellular single-unit recording methods. In: Boulton A, Baker G, Vanderwolf C, editors. Neurophysiological techniques. Humana Press; 1991. p. 1–64.
[59] Claverol-Tinture E, Pine J. Extracellular potentials in low-density dissociated neuronal cultures. J Neurosci Methods 2002;117:13–21.
[60] Bulai PM, Molchanov PG, Denisov AA, Pitlik TN, Cherenkevich SN. Extracellular electrical signals in a neuron-surface junction: model of heterogeneous membrane conductivity. Eur Biophys J Biophys Lett 2012;41:319–27.
[61] Thakore V, Molnar P, Hickman JJ. An optimization-based study of equivalent circuit models for representing recordings at the neuron-electrode interface. IEEE Trans Biomed Eng 2012;59:2338–47.
[62] Ingebrandt S, Wrobel G, Zhang Y, Meyburg S, Schindler M, Sommerhage F, et al. Investigation of extracellular signal shapes recorded by planar metal micro electrodes and field-effect transistors. Sensors, 2005 IEEE; 2005 611–6.
[63] Nitzan H, Mark S-I, Yael H. Optical validation of in vitro extra-cellular neuronal recordings. J Neural Eng 2011;8:056008.
[64] Heimburg T. The capacitance and electromechanical coupling of lipid membranes close to transitions: the effect of electrostriction. Biophys J 2012;103:918–29.
[65] Sabri S, Soler M, Foa C, Pierres A, Benoliel A, Bongrand P. Glycocalyx modulation is a physiological means of regulating cell adhesion. J Cell Sci 2000;113:1589–600.
[66] Sorribas H, Braun D, Leder L, Sonderegger P, Tiefenauer L. Adhesion proteins for a tight neuron–electrode contact. J Neurosci Methods 2001;104:133–41.
[67] Gao L, Lipowsky HH. Composition of the endothelial glycocalyx and its relation to its thickness and diffusion of small solutes. Microvasc Res 2010;80:394–401.
[68] Ebong EE, Macaluso FP, Spray DC, Tarbell JM. Imaging the endothelial glycocalyx in vitro by rapid freezing/freeze substitution transmission electron microscopy. Arterioscler Thromb Vasc Biol 2011;31:1908–15.
[69] Blau A, Weinl C, Mack J, Kienle S, Jung G, Ziegler C. Promotion of neural cell adhesion by electrochemically generated and functionalized polymer films. J Neurosci Methods 2001;112:65–73.
[70] Wrobel G, Höller M, Ingebrandt S, Dieluweit S, Sommerhage F, Bochem HP, et al. Transmission electron microscopy study of the cell–sensor interface. J R Soc Interface 2008;5:213–22.
[71] Braun D, Fromherz P. Fluorescence interferometry of neuronal cell adhesion on microstructured silicon. Phys Rev Lett 1998;81:5241–4.
[72] Kotov NA, Winter JO, Clements IP, Jan E, Timko BP, Campidelli S, et al. Nanomaterials for neural interfaces. Adv Mater 2009;21:3970–4004.
[73] Arcot Desai S, Rolston JD, Guo L, Potter SM. Improving impedance of implantable microwire multi-electrode arrays by ultrasonic electroplating of durable platinum black. Front Neuroeng 2010;3.
[74] Kim R, Hong N, Nam Y. Gold nanograin microelectrodes for neuroelectronic interfaces. Biotechnol J 2013;8:206–14.
[75] Graham AHD, Bowen CR, Taylor J, Robbins J. Neuronal cell biocompatibility and adhesion to modified CMOS electrodes. Biomed Microdevices 2009;11:1091–101.
[76] Moxon KA, Hallman S, Aslani A, Kalkhoran NM, Lelkes PI. Bioactive properties of nanostructured porous silicon for enhancing electrode to neuron interfaces. J Biomater Sci Polym Ed 2007;18:1263–81.
[77] Hai A, Dormann A, Shappir J, Yitzchaik S, Bartic C, Borghs G, et al. Spine-shaped gold protrusions improve the adherence and electrical coupling of neurons with the surface of micro-electronic devices. J R Soc Interface 2009;6:1153–65.
[78] Spira ME, Hai A. Multi-electrode array technologies for neuroscience and cardiology. Nat Nanotechnol 2013;8:83–94.
[79] Van Meerbergen B, Raemaekers T, Winters K, Braeken D, Bartic C, Engelborghs Y, et al. On chip induced phagocytosis for improved neuronal cell adhesion. NSTI Nanotechnology Conference and Trade Show. Boston 2006; 2006. p. 107–10.
[80] Robinson JT, Jorgolli M, Shalek AK, Yoon M-H, Gertner RS, Park H. Vertical nanowire electrode arrays as a scalable platform for intracellular interfacing to neuronal circuits. Nat Nanotechnol 2012;7:180–4.
[81] Duan X, Gao R, Xie P, Cohen-Karni T, Qing Q, Choe HS, et al. Intracellular recordings of action potentials by an extracellular nanoscale field-effect transistor. Nat Nanotechnol 2012;7:174–9.
[82] Almquist BD, Melosh NA. Fusion of biomimetic stealth probes into lipid bilayer cores. Proc Natl Acad Sci 2010;107:5815–20.
[83] Kwiat M, Stein D, Patolsky F. Nanotechnology meets electrophysiology. Curr Opin Biotechnol 2012 (epub).
[84] Gross GW. Internal dynamics of randomized mammalian neuronal networks in culture. New York: Academic Press; 1994 .
[85] Moxon K, Hallman S, Sundarakrishnan A, Wheatley M, Nissanov J, Barbee K. Long-term recordings of multiple, single-neurons for clinical applications: the emerging role of the bioactive microelectrode. Materials 2009;2:1762–94.
[86] García AJ. Interfaces to control cell-biomaterial adhesive interactions. Polymers for regenerative medicine; 2006 171–90.
[87] Geiger B, Spatz JP, Bershadsky AD. Environmental sensing through focal adhesions. Nat Rev Mol Cell Biol 2009;10:21–33.
[88] Moore SW, Sheetz MP. Biophysics of substrate interaction: influence on neural motility, differentiation, and repair. Dev Neurobiol 2011;71:1090–101.
[89] Boehler MD, Leondopulos SS, Wheeler BC, Brewer GJ. Hippocampal networks on reliable patterned substrates. J Neurosci Methods 2012;203:344–53.
[90] Grier DG. A revolution in optical manipulation. Nature 2003;424:810–6.
[91] Berns MW. A history of laser scissors (microbeams). Methods Cell Biol 2007;82:1–58.
[92] Difato F, Tsushima H, Pesce M, Benfenati F, Blau A, Chieregatti E. The formation of actin waves during regeneration after axonal lesion is enhanced by BDNF. Sci Rep 2011;1 (AdvPub).
[93] Maher MP, Pine J, Wright J, Tai YC. The neurochip: a new multielectrode device for stimulating and recording from cultured neurons. J Neurosci Methods 1999;87:45–56.
[94] Zeck G, Fromherz P. Noninvasive neuroelectronic interfacing with synaptically connected snail neurons immobilized on a semiconductor chip. Proc Natl Acad Sci U S A 2001;98:10457–62.
[95] Merz M, Fromherz P. Silicon chip interfaced with a geometrically defined net of snail neurons. Adv Funct Mater 2005;15:739–44.
[96] Suzuki I, Sugio Y, Jimbo Y, Yasuda K. Stepwise pattern modification of neuronal network in photo-thermally-etched agarose architecture on multi-electrode array chip for individual-cell-based electrophysiological measurement. Lab Chip 2005;5:241–7.
[97] Erickson J, Tooker A, Tai YC, Pine J. Caged neuron MEA: a system for long-term investigation of cultured neural network connectivity. J Neurosci Methods 2008;175:1–16.
[98] Kim W, Ng JK, Kunitake ME, Conklin BR, Yang P. Interfacing silicon nanowires with mammalian cells. J Am Chem Soc 2007;129:7228–9.
[99] Hällström W, Mårtensson T, Prinz C, Gustavsson P, Montelius L, Samuelson L, et al. Gallium phosphide nanowires as a substrate for cultured neurons. Nano Lett 2007;7:2960–5.
[100] Pearce TM, Williams JC. Microtechnology: meet neurobiology. Lab Chip 2007;7:30–40.
[101] Wang L, Riss M, Buitrago JO, Claverol-Tinturé E. Biophysics of microchannel-enabled neuron–electrode interfaces. J Neural Eng 2012;9:026010.
[102] Pataky K, Braschler T, Negro A, Renaud P, Lutolf MP, Brugger J. Microdrop printing of hydrogel bioinks into 3D tissue-like geometries. Adv Mater 2011;24:391–6.
[103] Christelle P, Waldemar H, Thomas M, Lars S, Lars M, Martin K. Axonal guidance on patterned free-standing nanowire surfaces. Nanotechnology 2008;19:345101.
[104] Liangbin P, Sankaraleengam A, Eric F, Gregory JB, Bruce CW. Propagation of action potential activity in a predefined microtunnel neural network. J Neural Eng 2011;8:046031.
[105] Fitzgerald JJ, Lacour SP, McMahon SB, Fawcett JW. Microchannels as axonal amplifiers. IEEE Trans Biomed Eng 2008;55:1136–46.
[106] Taylor AM, Dieterich DC, Ito HT, Kim SA, Schuman EM. Microfluidic local perfusion chambers for the visualization and manipulation of synapses. Neuron 2010;66:57–68.
[107] Ziolkowska K, Kwapiszewski R, Brzozka Z. Microfluidic devices as tools for mimicking the in vivo environment. New J Chem 2011;35:979–90.
[108] Dworak BJ, Wheeler BC. Novel MEA platform with PDMS microtunnels enables the detection of action potential propagation from isolated axons in culture. Lab Chip 2009;9:404–10.
[109] Greiner AM, Richter B, Bastmeyer M. Micro-engineered 3D scaffolds for cell culture studies. Macromol Biosci 2012;12:1301–14.
[110] Cai L, Zhang L, Dong J, Wang S. Photocured biodegradable polymer substrates of varying stiffness and microgroove dimensions for promoting nerve cell guidance and differentiation. Langmuir 2012;28:12557–68.
[111] Rajput D, Crowder SW, Hofmeister L, Costa L, Sung H-J, Hofmeister W. Cell interaction study method using novel 3D silica nanoneedle gradient arrays. Colloids Surf B Biointerfaces 2013;102:111–6.
[112] Alves NM, Pashkuleva I, Reis RL, Mano JF. Controlling cell behavior through the design of polymer surfaces. Small 2010;6:2208–20.
[113] Greve F, Lichtenberg J, Kirstein KU, Frey U, Perriard JC, Hierlemann A. A perforated CMOS microchip for immobilization and activity monitoring of electrogenic cells. J Micromech Microeng 2007;17:462.
[114] Heida T, Rutten WLC, Marani E. Understanding dielectrophoretic trapping of neuronal cells: modelling electric field, electrode-liquid interface and fluid flow. J Phys D: Appl Phys 2002;35:1592.
[115] Jaber FT, Labeed FH, Hughes MP. Action potential recording from dielectrophoretically positioned neurons inside micro-wells of a planar microelectrode array. J Neurosci Methods 2009;182:225–35.
[116] Ma Z, Pirlo R, Yun J, Peng X, Yuan X, Gao B. Laser guidance-based cell micropatterning. In: Ringeisen BR, Spargo BJ, Wu PK, editors. Cell and organ printing. Netherlands: Springer; 2010. p. 137–59.

[117] Chiou PY, Ohta AT, Wu MC. Massively parallel manipulation of single cells and microparticles using optical images. Nature 2005;436:370–2.
[118] Kaehr B, Allen R, Javier DJ, Currie J, Shear JB. Guiding neuronal development with in situ microfabrication. Proc Natl Acad Sci U S A 2004;101:16104–8.
[119] Chiu DT, Li Jeon N, Huang S, Kane RS, Wargo CJ, Choi IS, et al. Patterned deposition of cells and proteins onto surfaces by using three-dimensional microfluidic systems. Proc Natl Acad Sci U S A 2000;97:2408–13.
[120] Boland T, Xu T, Damon B, Cui X. Application of inkjet printing to tissue engineering. Biotechnol J 2006;1:910–7.
[121] Ferris C, Gilmore K, Wallace G, Panhuis M. Biofabrication: an overview of the approaches used for printing of living cells. Appl Microbiol Biotechnol 2013;97:4243–58.
[122] Wang X, Hayes JA, Picardo MC, Del Negro CA. Automated cell-specific laser detection and ablation of neural circuits in neonatal brain tissue. J Physiol 2013 May 15;591(Pt 10):2393–401.
[123] Ehrlicher A, Betz T, Stuhrmann B, Koch D, Milner V, Raizen MG, et al. Guiding neuronal growth with light. Proc Natl Acad Sci 2002;99:16024–8.
[124] Li N, Zhang X, Song Q, Su R, Zhang Q, Kong T, et al. The promotion of neurite sprouting and outgrowth of mouse hippocampal cells in culture by graphene substrates. Biomaterials 2011;32:9374–82.
[125] Bendali A, Hess LH, Seifert M, Forster V, Stephan A-F, Garrido JA, et al. Purified neurons can survive on peptide-free graphene layers. Adv Healthc Mater 2013;2(7):929–33.
[126] Ariano P, Lo Giudice A, Marcantoni A, Vittone E, Carbone E, Lovisolo D. A diamond-based biosensor for the recording of neuronal activity. Biosens Bioelectron 2009;24:2046–50.
[127] Mrksich M. A surface chemistry approach to studying cell adhesion. Chem Soc Rev 2000;29:267–73.
[128] Ziaie B, Baldi A, Atashbar M. Introduction to micro-/nanofabrication. In: Bhushan B, editor. Springer handbook of nanotechnology. Berlin Heidelberg: Springer; 2010. p. 231–69.
[129] Green RA, Lovell NH, Poole-Warren LA. Cell attachment functionality of bioactive conducting polymers for neural interfaces. Biomaterials 2009;30:3637–44.
[130] Muskovich M, Bettinger CJ. Biomaterials-based electronics: polymers and interfaces for biology and medicine. Adv Healthc Mater 2012;1:248–66.
[131] Kang K, Lee S, Kim R, Choi IS, Nam Y. Electrochemically driven, electrode-addressable formation of functionalized polydopamine films for neural interfaces. Angew Chem Int Ed 2012;51:13101–4.
[132] Yeo W-S, Mrksich M. Electroactive self-assembled monolayers that permit orthogonal control over the adhesion of cells to patterned substrates†. Langmuir 2006;22:10816–20.
[133] Qin D, Xia Y, Whitesides GM. Soft lithography for micro- and nanoscale patterning. Nat Protoc 2010;5:491–502.
[134] Zheng WF, Zhang W, Jiang XY. Precise control of cell adhesion by combination of surface chemistry and soft lithography. Adv Healthc Mater 2013;2:95–108.
[135] Fricke R, Zentis PD, Rajappa LT, Hofmann B, Banzet M, Offenhäusser A, et al. Axon guidance of rat cortical neurons by microcontact printed gradients. Biomaterials 2011;32:2070–6.
[136] Nam Y, Branch DW, Wheeler BC. Epoxy-silane linking of biomolecules is simple and effective for patterning neuronal cultures. Biosens Bioelectron 2006;22:589–97.
[137] Fukuda J, Khademhosseini A, Yeh J, Eng G, Cheng J, Farokhzad OC, et al. Micropatterned cell co-cultures using layer-by-layer deposition of extracellular matrix components. Biomaterials 2006;27:1479–86.
[138] Krogh M, Asberg P. My little guide to soft lithography. Soft lithography for dummies. Linköping University; 2003 15.
[139] Shadpour H, Allbritton NL. In situ roughening of polymeric microstructures. ACS Appl Mater Interfaces 2010;2:1086–93.
[140] Reyes DR, Perruccio EM, Becerra SP, Locascio LE, Gaitan M. Micropatterning neuronal cells on polyelectrolyte multilayers. Langmuir 2004;20:8805–11.
[141] Didar TF, Foudeh AM, Tabrizian M. Patterning multiplex protein microarrays in a single microfluidic channel. Anal Chem 2011;84:1012–8.
[142] Blau A, Ugniwenko T. Induction and analysis of cell adhesion and differentiation on inkjet micropatterned substrates. Phys Status Solidi C 2007;4:1873–6.
[143] Clark P, Britland S, Connolly P. Growth cone guidance and neuron morphology on micropatterned laminin surfaces. J Cell Sci 1993;105:203–12.
[144] Sorribas H, Padeste C, Tiefenauer L. Photolithographic generation of protein micropatterns for neuron culture applications. Biomaterials 2002;23:893–900.
[145] Yamaguchi M, Ikeda K, Suzuki M, Kiyohara A, Kudoh SN, Shimizu K, et al. Cell patterning using a template of microstructured organosilane layer fabricated by vacuum ultraviolet light lithography. Langmuir 2011;27:12521–32.
[146] Slater JH, Miller JS, Yu SS, West JL. Fabrication of multifaceted micropatterned surfaces with laser scanning lithography. Adv Funct Mater 2011;21:2876–88.
[147] Cheng J, Zhu G, Wu L, Du X, Zhang H, Wolfrum B, et al. Photopatterning of self-assembled poly (ethylene) glycol monolayer for neuronal network fabrication. J Neurosci Methods 2013;213:196–203.
[148] Rutten WL, Ruardij TG, Marani E, Roelofsen BH. Neural networks on chemically patterned electrode arrays: towards a cultured probe. Acta Neurochir Suppl 2007;97:547–54.
[149] Curley JL, Jennings SR, Moore MJ. Fabrication of micropatterned hydrogels for neural culture systems using dynamic mask projection photolithography. J Vis Exp 2011:e2636.
[150] Lakard S, Herlem G, Propper A, Kastner A, Michel G, Valles-Villarreal N, et al. Adhesion and proliferation of cells on new polymers modified biomaterials. Bioelectrochemistry 2004;62:19–27.
[151] Kleinman HK, McGarvey ML, Liotta LA, Robey PG, Tryggvason K, Martin GR. Isolation and characterization of type IV procollagen, laminin, and heparan sulfate proteoglycan from the EHS sarcoma. Biochemistry 1982;21:6188–93.
[152] Young S, Wong M, Tabata Y, Mikos AG. Gelatin as a delivery vehicle for the controlled release of bioactive molecules. J Control Release 2005;109:256–74.
[153] Huang Y, Onyeri S, Siewe M, Moshfeghian A, Madihally SV. In vitro characterization of chitosan–gelatin scaffolds for tissue engineering. Biomaterials 2005;26:7616–27.
[154] Morla A, Zhang Z, Ruoslahti E. Superfibronectin is a functionally distinct form of fibronectin. Nature 1994;367:193–6.
[155] Massia SP, Holecko MM, Ehteshami GR. In vitro assessment of bioactive coatings for neural implant applications. J Biomed Mater Res A 2004;68:177–86.
[156] Preissner KT. Structure and biological role of vitronectin. Annu Rev Cell Biol 1991;7:275–310.
[157] Stoeckli ET, Kuhn TB, Duc CO, Ruegg MA, Sonderegger P. The axonally secreted protein axonin-1 is a potent substratum for neurite growth. J Cell Biol 1991;112:449–55.
[158] Kleinman HK, Luckenbill-Edds L, Cannon FW, Sephel GC. Use of extracellular matrix components for cell culture. Anal Biochem 1987;166:1–13.
[159] Lanza R, Langer R, Vacanti JP. Principles of tissue engineering. Academic press; 2011 .
[160] Tian B, Cohen-Karni T, Qing Q, Duan X, Xie P, Lieber CM. Three-dimensional, flexible nanoscale field-effect transistors as localized bioprobes. Science 2010;329:830–4.